NASA TECHNICAL NOTE

NASA TN D-3000

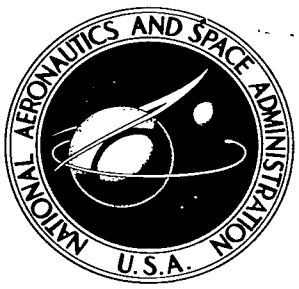

NASA TN D-3000

BANDWIDTH OPTIMIZATION FOR FREQUENCY SHIFT KEYING

by James C. Morakis

Goddard Space Flight Center
Greenbelt, Md.

NATIONAL AERONAUTICS AND SPACE ADMINISTRATION • WASHINGTON, D. C. • SEPTEMBER 1965

NASA TN D-3000

BANDWIDTH OPTIMIZATION FOR FREQUENCY SHIFT KEYING

By James C. Morakis

Goddard Space Flight Center
Greenbelt, Md.

NATIONAL AERONAUTICS AND SPACE ADMINISTRATION

For sale by the Clearinghouse for Federal Scientific and Technical Information
Springfield, Virginia 22151 – Price $2.00

BANDWIDTH OPTIMIZATION FOR FREQUENCY SHIFT KEYING

by
James C. Morakis
Goddard Space Flight Center

SUMMARY

The behavior of a frequency shift keying detector as a function of bandwidth has been analyzed for four types of bandpass filters, and bit error probability curves have been plotted for each of the four filters with the bandwidth as the variable. The four filters are: (a) a dump type, (b) a sharp type, (c) a combination of a and b, and (d) a singly tuned high Q filter. The purpose of this paper is to bring out the variation of optimum bandwidth as the assumptions about the system vary. Another significant result is the unbalance of the probability of error due to different binary combinations, and consequently, the dependence of the average probability of error on just the probability of error of two out of 2^k combinations.

CONTENTS

Summary iii

INTRODUCTION 1

SYSTEM DESCRIPTION 2

THE EFFECT OF BANDWIDTH ON THE DIFFERENT TYPES OF INTERFERENCE 2

Effect of Bandwidth on Intersymbol Interference 3

The Effect of Bandwidth on Noise and Crosstalk. 4

Description of the Different Outputs 5

Assumptions 6

BANDWIDTH OPTIMIZATION 7

Expressions for the Probability of Error 7

Generalized Signals at the Detector Output 8

Generation of the Four Types of Filters. 10

Comparative Performance of the Four Filters 12

DISCUSSION 13

CONCLUSIONS 15

References 16

Bibliography 16

Appendix A—A Low-Pass to Band-Pass Filter Equivalence 19

Appendix B—The Step Response of a Singly-Tuned Circuit 25

Appendix C—Generalized Filter Outputs in the FSK System 29

Appendix D—Comparator Output Signal-to-Noise Ratios 33

Appendix E—Formulation of the Expressions Governing A Singly Tuned Circuit 35

Appendix F—Definitions 37

BANDWIDTH OPTIMIZATION FOR FREQUENCY SHIFT KEYING

by
James C. Morakis
Goddard Space Flight Center

INTRODUCTION

The bit error probability at the output of a frequency shift keying (FSK) receiver of the type shown in Figure 1 is $\frac{1}{2}\left(e^{-E/2N_0}\right)$ (Reference 1) under the following assumptions:

a. The noise is white Gaussian.

b. The mark and space frequencies are sufficiently separated so that the cross-correlation between any two of the two signals and the noise in the two filters is zero.

c. The filters are exactly matched. (These filters have an output which is proportional to the cross-correlation of the inverse in time of the filter impulse response which must be made equal to the expected waveform.)

d. The detector is an envelope detector which follows the envelope and the signal very closely.

e. The type of FSK (continuous or discontinuous phase at the time of frequency change) is not specified.

f. The S/N is large.

g. The filters are free of intersymbol interference.

In an actual system most of these assumptions are approximately valid, but some assumptions are completely unjustifiable. Consequently, for most practical systems, the above quoted bit error probability is a lower bound.

It is possible to choose some of the parameters in such a manner so as to optimize the system, but there are some parameters which are contradictory. For example, let us take assumption (c) which states that the filters are matched. A matched filter for FSK implies two filters centered at frequencies f_1

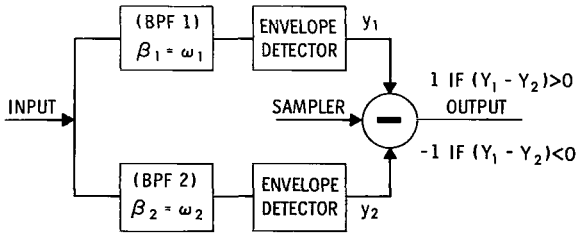

Figure 1—The FSK detector.

and f_2, respectively, provided the separation of these two frequencies is large enough to reduce the interchannel interference to zero.

Furthermore, the filter bandwidth, B, is assumed to be small to reduce the noise and crosstalk and yet not too small to cause signal distortion (intersymbol interference). This paper shall retain the assumptions that can be readily justified; and varying the remaining assumptions we shall generate four different types of filters.

Succeeding sections of this paper will describe the system, and present a preliminary glimpse of the problem, by investigating the effects of bandwidth on each of the different types of interference (considering the remaining interferences as nonexistent). This preliminary simple analysis will serve two objectives: (a) the knowledge of the range of some variables that will enable us to make some realistic assumptions, and (b) a better insight into the problem.

Following the bandwidth effect investigation is a section devoted to the derivation of the bit error probability as a function of the $(S/N)_{in}$ and the filter characteristics for the four different filter types. Throughout the text the variable πBT is used. However, if T is given, B may be found for any given value of πBT.

SYSTEM DESCRIPTION

The system under consideration is shown in Figure 1. The filters are high Q singly tuned circuits; however, by varying their bandwidth, shape and center frequency, we will effectively obtain four types of filters. In any of these types, the envelope detectors employ full wave rectifiers, and the comparator compares the two outputs at the sampling instant as dictated by the sampler output, which occurs at the maximum signal to interference ratio.

We will frequently reach a point where some complexities may be simplified if we know the dynamic range of some variables involved. To gain this knowledge some preliminary analyses must be conducted under simplified conditions.

THE EFFECT OF BANDWIDTH ON DIFFERENT TYPES OF INTERFERENCE

The three main types of interference are noise, intersymbol and interchannel (crosstalk), and although their sources are varied, these quantities depend on one common variable, the bandwidth. For example, the noise power N is given by:

$$N = \int_{-\infty}^{\infty} N_0 \left|H(\omega)\right|^2 d\omega \approx BN_0$$

where N_0, a constant (assuming white noise), is the noise power per unit bandwidth (cycle), and B is the 3-db bandwidth of the bandpass filter, or the bandwidth of the equivalent rectangular filter so far as noise power is concerned.

The crosstalk is of the form Signal/D_i where

$$D_i^2 = \left[\left(\frac{\omega_i}{\omega_j} + 1\right)\frac{n}{BT}\right]^2 + 1$$

$$(i \neq j, \quad i, j = 1, 2) \tag{1a}$$

and the intersymbol interference is measured by the "spread beyond the bit period" of the impulse response of the equivalent low-pass filter. This is shown to be (Appendix A)

$$Ce^{-\pi BT}$$

where C is a proportionality constant and B is the 3-db bandwidth.

Since the effects of bandwidth variation on adjacent channel, noise, and intersymbol interference are opposing, it will be necessary to study those effects separately by assuming only one interference at a time.

Effect of Bandwidth on Intersymbol Interference

The response of a singly tuned bandpass filter and envelope detector combination to an amplitude modulated step signal of the form $U(t)\sin\omega t$ is (Appendix B)

$$y(t) = \left\{\frac{\left(1 - \frac{\beta_0}{\beta}\, e^{-\pi BT}\right)^2 + 4\,\frac{\beta_0}{\beta}\, e^{-\pi BT} \sin\left[(\beta - \omega)\, t + \psi - \phi\right]}{\left(\frac{\beta_0^2 - \omega^2}{2\pi B\omega}\right)^2 + 1}\right\}. \tag{1b}$$

For $\beta_0 = \beta$ and $\omega = \beta_0$, (or no frequency offset), Equation 1b becomes:

$$y(t) = 1 - e^{-\pi BT} \tag{1c}$$

Note that this result is identical to the one which would have been obtained if the result of Appendix A was used.

Assuming *no crosstalk* and *no noise*, the signal at the outputs of the two filters is shown in Figure 2 for the four cases of a 3-bit signal in improving order. These sketches demonstrate the effect of intersymbol interference alone, for BT = 0.41.

The calculation of the difference of the outputs of the mark and space envelopes depends on the type of sequence received. For example, the four cases (in order of improvement) for the 3-bit words of Figure 2 are listed below.

Table 1

Three-bit Words at Detector Outputs.

Sequence		Difference Between M&S Detector $(y_1 - y_2)$
a	001 or 110	$1 - 2\exp(-\pi BT) + \exp(-3\pi BT)$
b	101 or 010	$1 - 2\exp(-\pi BT) + 2\exp(-2\pi BT) - \exp(-3\pi BT)$
c	011 or 100	$1 - 2\exp(-2\pi BT) + \exp(-3\pi BT)$
d	111 or 000	$1 - 2\exp(-3\pi BT)$

To optimize the system for the worst case, replace $K(y_1 - y_2)/N$ by the expression of Equation 2 and then obtain the maximum of that expression which occurs at $\pi BT = 2.5$. This result may be checked by observing the maximum of curve 3 in Figure 3.

$$y_1 - y_2 = C\left(1 - 2e^{-\pi BT} + e^{-3\pi BT}\right) \qquad (2)$$

The Effect of Bandwidth on Noise and Crosstalk

When the intersymbol interference is zero,* the noise and crosstalk are proportional to the bandwidth so the S/N increases as B decreases.

This effect is illustrated in Figure 3 where the expression of Equation 3a representing this case is plotted as curve 1.

$$y_1 - y_2 = C\left(1 - e^{-\pi BT}\right)\left(1 - \frac{1}{D}\right)\sqrt{B} \qquad (3a)$$

*This is true if the filter is of the integrate and dump type.

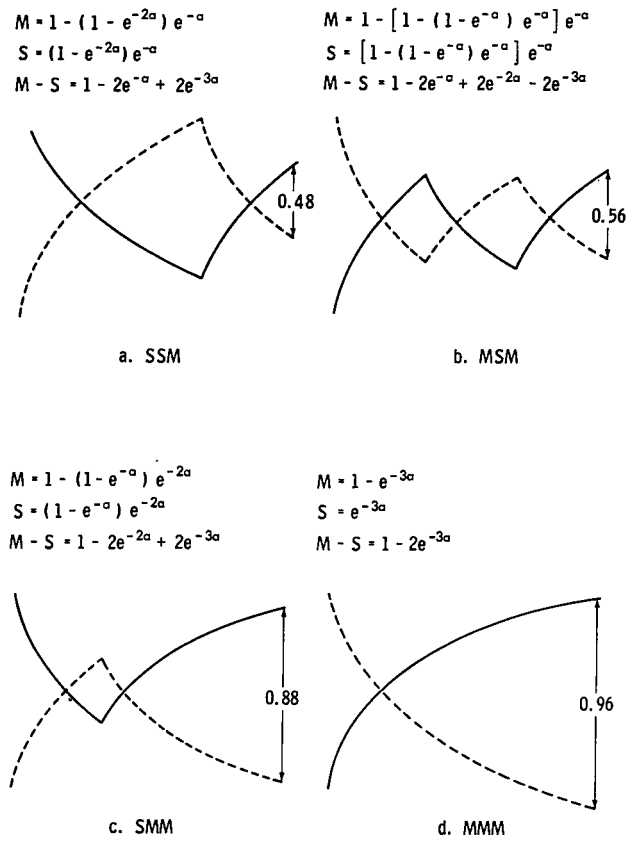

Figure 2—Approximate waveforms at the output of mark (solid line) and space (broken line) detectors and their difference for three-bit words. (a) SSM. (b) MSM. (c) SMM. (d) MMM.

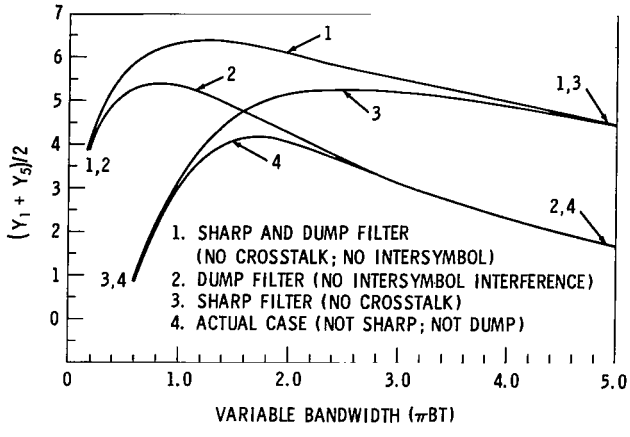

Figure 3—The plot of $1/2\ (Y_1 + Y_5)$ vs. πBT.

Description of the Different Outputs

When a sequence of zeros and ones (each represented by one of the frequencies f_1, f_2) is applied to the mark filter, the output will be a mixture of f_1, f_2, β_1 and their cross products. One is then confronted with the problem of finding the envelope of the sum of waveforms of different frequencies. The two difficulties in this problem are: (a) the nonlinearity of the envelope detector and (b) the sensitivity of the output on the relative phase of the different input frequencies.

This section is devoted to the solution of the dynamic range of some of the variables so that valid assumptions may be made in a later part of this section. Therefore, let us now define and obtain expressions for the different signals that contribute to the output of the detector.

The response of the mark filter to a mark signal applied at $t = 0$ is the main signal, and it is represented by $y_{1,1,0}$*. The amplitude of the main response is obtained by setting $\omega = \beta = \omega_1$ in Equation B9 or using Equation B10 of Appendix B.

$$y_{1,1,0} \approx 1 - de^{-\pi BT}; \quad d \approx 1 \tag{3b}$$

The response of the space filter to a mark signal applied at $t = 0$ is the crosstalk, which is represented by $y_{0,1,0}$; and its amplitude fluctuates between the two extreme values of

$$y_{0,1,0} = \frac{1 \pm de^{-\pi BT}}{D} . \tag{3c}$$

This has a frequency

$$\left|\frac{\beta_2 - \omega_1}{2\pi}\right| = nf_D , \tag{3d}$$

where D is the crosstalk factor defined in Equation 8e, and f_D is the data bit frequency.

The response of the mark filter to mark signals applied at $t < 0$ is the crosstalk and is [from Equation B11 with $t = -(k+1)T$]:

$$y_{1,1,-k} = \left(1 - de^{-\pi BT}\right) de^{-\pi BkT} . \tag{3e}$$

*For $y_{i,j,k}$: i = 1,0 and refers to the mark (1) and space (0) filters.
j = 1,0 and refers to the mark (1) and space (0) signals.
k = $-\infty, \cdots, -2, -1, 0$ and refers to the sampling interval.

Finally, the response of the mark filter to a space signal applied at $t < 0$ is called the crosstalk intersymbol interference; and its amplitude fluctuates between the two values:

$$y_{0,1,-k} = \frac{1 \pm de^{-\pi BT}}{D} de^{-\pi BkT} . \tag{3f}$$

When k is an integer, the sampling may occur at the minimum of the expression for crosstalk, thus reducing the expressions to ones involving only the negative sign. Four more definitions may be generated from the above definitions by interchanging the words "Mark" and "Space."

Treating the effects of the mark and space frequencies as two vectors of comparable amplitude but different frequency; the average value of the resulting vector is the square root of the sum of the squares, since the two vectors are orthogonal. This is, incidentally, the justification for the form of Equations C7 and C8 of Appendix C.

Assumptions

The preliminary analysis of this section has revealed the following results:

a. Under no crosstalk assumptions, (equivalent square filter), the optimum value of πBT is between .6 and 2.6. However, since the optimum value of πBT for the worst case is 2.5, we will assume πBT to be no larger than 2.5.

b. The effect of intersymbol interference will be far more serious than that of crosstalk for the filters that will give the value of BT discussed in (a).

In view of the above results we choose to make the following assumption for later analysis:

a. The noise is white Gaussian.

b. The mark and space frequencies are separated by an amount equal to nf_D. If this spacing is further increased, the probability of error will be lowered, the crosstalk will be lowered, and the optimum bandwidth will occur at a higher value of πBT.

c. The filters are singly tuned high Q filters located at $\beta_1 = 2\pi f_1$ and $\beta_2 = 2\pi f_2$.

d. The envelope detector follows the envelope of the signal very closely (a full wave rectifier helps).

e. The change in subcarrier frequency occurs at the zero crossings.

f. The signal-to-noise ratio is fairly large to justify the use of the following expression (Reference 2) in this system:

$$P_e = \frac{1}{2} e^{-cE/2N_0} \tag{4}$$

BANDWIDTH OPTIMIZATION

Expressions for the Probability of Error

The objective of bandwidth optimization will be pursued by minimizing the probability of error. This, however, is a function of the signal-to-noise ratio, and this ratio depends on the input sequences.* The probability of error (P_e) for a given sequence is given by:

$$P_e = P(M)\,P \text{ (an M will be detected as an S)} + P(S)\,P \text{ (an S will be detected as an M)} \quad (5)$$

The average probability of error for K admissible sequences is then:

$$P_{ave.} = \sum_{i=1}^{K} P\left(i^{th} \text{ sequence}\right)\left(P_e\right)_i \,. \quad (6a)$$

If all the binary sequences of length k are admissible, Equation 6a becomes

$$P_{ave.} = \frac{1}{2^k} \sum_{i=1}^{2^k} \left(P_e\right)_i \,. \quad (6b)$$

Equation 6 is a summation of 2^k terms where k is the filter memory in bits. Theoretically, k should be infinite, but for the time constants found previously, $(1.6 < \pi BT)$, k should not be larger than 3. So for $k = 3$ we obtain the 3-bit sequences identical to those in Table 1.

For $P(M) = P(S) = 1/2$, $P(M/S) = P(S/M)$, and large S/N, the bit error probability for noncoherent FSK is given by Equation (4) with $c = 1/BT$, the reciprocal of the bit period-noise bandwidth product. The system becomes optimum by setting $B = 1/T$; this maximizes the S/N and reduces the expression of Equation (4) to the familiar

$$\frac{1}{2} e^{-E/2N_0} \quad (4)$$

where E is the signal energy per bit and N_0 is the one sided noise spectral density.

*This effect may be observed in Figure 2.

We shall optimize B by keeping E_{in}/N_0 a parameter, and T constant. The exponent then becomes

$$\frac{E_{out}}{2N_0}\frac{1}{BT} = \frac{\pi}{2}\frac{E_{in}}{N_0}\left(\frac{y_1 - y_2}{\sqrt{\pi BT}}\right)^2 ,$$

where $E_{in}(y_1 - y_2)^2 = E_{out}$ at the k^{th} sampling instant $(t = kT)$.

Returning to Equation 6, we find that it expands to the form (using $k = 3$)

$$\langle P \rangle = \frac{1}{2^k}\sum_{i=1}^{2^k}(P_e)_i = \frac{1}{8}\sum_{i=1}^{8}P_i = \frac{1}{8}\sum_{i=1}^{8}\frac{1}{2}e^{-\pi/2(E_{in}/N_0)Y_i^2} , \tag{7}$$

where

$$Y_i = \frac{y_1 - y_2}{\sqrt{\pi BT}} . \tag{8a}$$

Generalized Signals at the Detector Output

Since $y_1 - y_2$ will vary for each of the 2^k (8 in this case) inputs, we must calculate Y_i for each input. For $k = 3$, the inputs are:

Input number 1 is 001
Input number 2 is 101
Input number 3 is 011
Input number 4 is 111
Input number 5 is 110
Input number 6 is 010
Input number 7 is 100
Input number 8 is 000

Now using Equation C7 of Appendix C we generate Equation 8b that expresses the eight generalized outputs corresponding to the above inputs.*

$$\left.\begin{aligned}
Y_1 &= f(y_{1,0,-2}, y_{1,0,-1}, y_{1,1,0}) - f(y_{2,0,-2}, y_{2,0,-1}, y_{2,1,0}) \\
Y_2 &= f(y_{1,1,-2}, y_{1,0,-1}, y_{1,1,0}) - f(y_{2,1,-2}, y_{2,0,-1}, y_{2,1,0}) \\
Y_3 &= f(y_{1,0,-2}, y_{1,1,-1}, y_{1,1,0}) - f(y_{2,0,-2}, y_{2,1,-1}, y_{2,1,0}) \\
Y_4 &= f(y_{1,1,-2}, y_{1,1,-1}, y_{1,1,0}) - f(y_{2,1,-2}, y_{2,1,-1}, y_{2,1,0}) \\
Y_5 &= f(y_{1,1,-2}, y_{1,1,-1}, y_{1,0,0}) + f(y_{2,1,-2}, y_{2,1,-1}, y_{2,0,0}) \\
Y_6 &= f(y_{1,0,-2}, y_{1,1,-1}, y_{1,0,0}) + f(y_{2,0,-2}, y_{2,1,-1}, y_{2,0,0}) \\
Y_7 &= f(y_{1,1,-2}, y_{1,0,-1}, y_{1,0,0}) + f(y_{2,1,-2}, y_{2,0,-1}, y_{2,0,0}) \\
Y_8 &= f(y_{1,0,-2}, y_{1,0,-1}, y_{1,0,0}) + f(y_{2,0,-2}, y_{2,0,-1}, y_{2,0,0})
\end{aligned}\right\} \tag{8b}$$

*$y_{q,r,s}$ is the output of the q filter due to a signal of type r applied s sampling periods ago.

$$
\left.
\begin{aligned}
Y_1 &= \frac{1 - d_1 e^{-a}}{\sqrt{a}} \left[d_1^2 \frac{\left(e^{-2a} + e^{-a}\right)^2}{D_1^2} + 1 \right]^{1/2} - \frac{1 - d_2 e^{-a}}{\sqrt{a}} \left[d_2^2 \left(e^{-2a} + e^{-a}\right)^2 + \frac{1}{D_2^2} \right]^{1/2} \\
Y_2 &= \frac{1 - d_1 e^{-a}}{\sqrt{a}} \left[\frac{d_1^2 \left(e^{-a}\right)^2}{D_1^2} + \left(1 + d_1 e^{-2a}\right)^2 \right]^{1/2} - \frac{1 - d_2 e^{-a}}{\sqrt{a}} \left[d_2^2 \left(e^{-a}\right)^2 + \frac{\left(1 + d_2 e^{-2a}\right)^2}{D_2^2} \right]^{1/2} \\
Y_3 &= \frac{1 - d_1 e^{-a}}{\sqrt{a}} \left[\frac{d_1^2 \left(e^{-2a}\right)^2}{D_1^2} + \left(1 + d_1 e^{-a}\right)^2 \right]^{1/2} - \frac{1 - d_2 e^{-a}}{\sqrt{a}} \left[d_2^2 \left(e^{-2a}\right)^2 + \frac{\left(1 + d_2 e^{-a}\right)^2}{D_2^2} \right]^{1/2} \\
Y_4 &= \frac{1 - d_1 e^{-a}}{\sqrt{a}} \left[1 + d_1 e^{-a} + d_1 e^{-2a} \right] - \frac{1 - d_2 e^{-a}}{\sqrt{a}} \left[\frac{1 + d_2 e^{-a} + d_2 e^{-2a}}{D_2} \right] \\
Y_5 &= \frac{1 - d_2 e^{-a}}{\sqrt{a}} \left[d_2^2 \frac{\left(e^{-a} + e^{-2a}\right)^2}{D_2^2} + 1 \right]^{1/2} - \frac{1 - d_1 e^{-a}}{\sqrt{a}} \left[d_1^2 \left(e^{-2a} + e^{-a}\right)^2 + \frac{1}{D_1^2} \right]^{1/2}
\end{aligned}
\right\} \quad (8c)
$$

$$
\left.
\begin{aligned}
Y_5 &= Y_1 \text{ (with subscripts 1 and 2 interchanged),} \\
Y_6 &= Y_2 \text{ (with subscripts 1 and 2 interchanged),} \\
Y_7 &= Y_3 \text{ (with subscripts 1 and 2 interchanged),} \\
Y_8 &= Y_4 \text{ (with subscripts 1 and 2 interchanged),}
\end{aligned}
\right\} \quad (8d)
$$

where

$$
\left.
\begin{aligned}
D_i &= \left[(m_i + 1)^2 \left(\frac{n\pi}{a}\right)^2 + 1 \right]^{1/2}, \qquad i = 1, 2 \\
a &= \pi B T, \\
m_1 &= \frac{\beta_1}{\omega_2}, \qquad m_2 = \frac{\beta_2}{\omega_1}, \\
\left(\beta_1 - \omega_2\right) &= \left(\omega_1 - \beta_2\right) = 2\pi f_D n, \\
d_i &= \frac{\beta_{0i}}{\beta_i}. \qquad i = 1, 2
\end{aligned}
\right\} \quad (8e)
$$

Generation of the Four Types of Filters

The particular results for each of the four filters may be obtained by using the results of Appendix D with $d_1 = d_2 = 1$.

Case 1: Dump Filter With Large Subcarrier Separation $(D_1, D_2 \gg 1)$

$$Y_i = \frac{1 - e^{-a}}{\sqrt{a}} \qquad \text{for} \quad i = 1, 2, 3, 4, 5, 6, 7, 8. \tag{9}$$

Case 2: Dump Filter

$$\left.\begin{aligned} Y_1 = Y_2 = Y_3 = Y_4 &= \frac{1 - e^{-a}}{\sqrt{a}} \left(1 - \frac{1}{D_2}\right), \\ Y_5 = Y_6 = Y_7 = Y_8 &= \frac{1 - e^{-a}}{\sqrt{a}} \left(1 - \frac{1}{D_1}\right). \end{aligned}\right\} \tag{10}$$

Case 3: Sharp Filter $(D_1, D_2 \gg 1$, *But No Dumping*$)$

$$\left.\begin{aligned} Y_1 = Y_5 &= \frac{1 - e^{-a}}{\sqrt{a}} \left(1 - e^{-a} - e^{-2a}\right), \\ Y_2 = Y_6 &= \frac{1 - e^{-a}}{\sqrt{a}} \left(1 - e^{-a} + e^{-2a}\right), \\ Y_3 = Y_7 &= \frac{1 - e^{-a}}{\sqrt{a}} \left(1 + e^{-a} - e^{-2a}\right), \\ Y_4 = Y_8 &= \frac{1 - e^{-a}}{\sqrt{a}} \left(1 + e^{-a} + e^{-2a}\right). \end{aligned}\right\} \tag{11}$$

Case 4: Singly Tuned Filter (Actual Case)

$$
\begin{aligned}
Y_1 &= \frac{1 - e^{-a}}{\sqrt{a}} \left\{ \left[\frac{\left(e^{-a} + e^{-2a}\right)^2}{D_1^2} + 1 \right]^{1/2} - \left[\left(e^{-a} + e^{-2a}\right)^2 + \frac{1}{D_2^2} \right]^{1/2} \right\}, \\
Y_2 &= \frac{1 - e^{-a}}{\sqrt{a}} \left\{ \left[\frac{\left(e^{-a}\right)^2}{D_1^2} + \left(1 + e^{-2a}\right)^2 \right]^{1/2} - \left[\left(e^{-a}\right)^2 + \frac{\left(1 + e^{-2a}\right)^2}{D_2^2} \right]^{1/2} \right\}, \\
Y_3 &= \frac{1 - e^{-a}}{\sqrt{a}} \left\{ \left[\frac{\left(e^{-2a}\right)^2}{D_1^2} + \left(1 + e^{-a}\right)^2 \right]^{1/2} - \left[\left(e^{-2a}\right)^2 + \frac{\left(1 + e^{-a}\right)^2}{D_2^2} \right]^{1/2} \right\}, \\
Y_4 &= \frac{1 - e^{-a}}{\sqrt{a}} \left(1 + e^{-a} + e^{-2a}\right) \left(1 - \frac{1}{D_2}\right), \\
Y_5 &= \frac{1 - e^{-a}}{\sqrt{a}} \left\{ \left[\frac{\left(e^{-a} + e^{-2a}\right)^2}{D_2^2} + 1 \right]^{1/2} - \left[\left(e^{-a} + e^{-2a}\right)^2 + \frac{1}{D_1^2} \right]^{1/2} \right\}, \\
Y_6 &= \frac{1 - e^{-a}}{\sqrt{a}} \left\{ \left[\frac{\left(e^{-a}\right)^2}{D_2^2} + \left(1 + e^{-2a}\right)^2 \right]^{1/2} - \left[\left(e^{-a}\right)^2 + \frac{\left(1 + e^{-2a}\right)^2}{D_1^2} \right]^{1/2} \right\}, \\
Y_7 &= \frac{1 - e^{-a}}{\sqrt{a}} \left\{ \left[\frac{\left(e^{-2a}\right)^2}{D_2^2} + \left(1 + e^{-a}\right)^2 \right]^{1/2} - \left[\left(e^{-2a}\right)^2 + \frac{\left(1 + e^{-a}\right)^2}{D_1^2} \right]^{1/2} \right\}, \\
Y_8 &= \frac{1 - e^{-a}}{\sqrt{a}} \left(1 + e^{-a} + e^{-2a}\right) \left(1 - \frac{1}{D_1}\right).
\end{aligned}
\tag{12}
$$

Comparative Performance of the Four Filters

The average probability of error for each of the four cases is:

Case 1: Dump Filter With Large Subcarrier Separation

Applying Equations 7 and 9, we find

$$\langle P \rangle = \frac{1}{2} e^{-c\gamma_i^2} . \tag{13a}$$

Case 2: Dump Filter

Applying Equations 7 and 10, we find

$$\langle P \rangle = \frac{1}{2}\left(\frac{1}{2} e^{-c\gamma_1^2} + \frac{1}{2} e^{-c\gamma_5^2}\right) = \frac{1}{2}\left(P_1 + P_5\right) . \tag{13b}$$

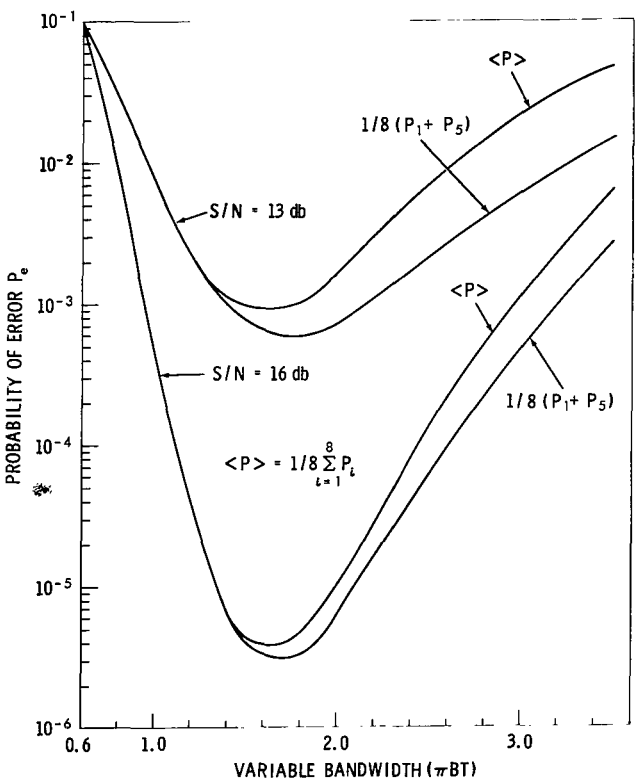

Figure 4—Probability of error P_e plotted against πBT for the singly tuned filter case.

Case 3: Sharp Filter

Using Equations 7 and 11, we find

$$\langle P \rangle = \frac{1}{2}\left[\frac{1}{4}\left(e^{-c\gamma_1^2} + e^{-c\gamma_2^2} + e^{-c\gamma_3^2} + e^{-c\gamma_4^2}\right)\right]$$

$$= \frac{1}{4}\left(P_1 + P_2 + P_3 + P_4\right) . \tag{14}$$

Case 4: Singly Tuned Filter

The use of Equations 7 and 12 does not simplify Equation 7 because in this case each γ is different. However, due to the exponential dependence of P_i on γ_i, the only significant γ's are the two smallest (Figures 4 and 5) i.e., γ_1 and γ_5 in cases 3 and 4. Consequently, for a <1.6 one may safely say than for all cases

$$\langle P \rangle = \frac{1}{2}\left(P_1 + P_5\right) = \frac{1}{4}\left(e^{-c\gamma_1^2} + e^{-c\gamma_5^2}\right) \tag{15}$$

if γ_1 and γ_5 are of comparable magnitudes, then one could obtain some insight as to the

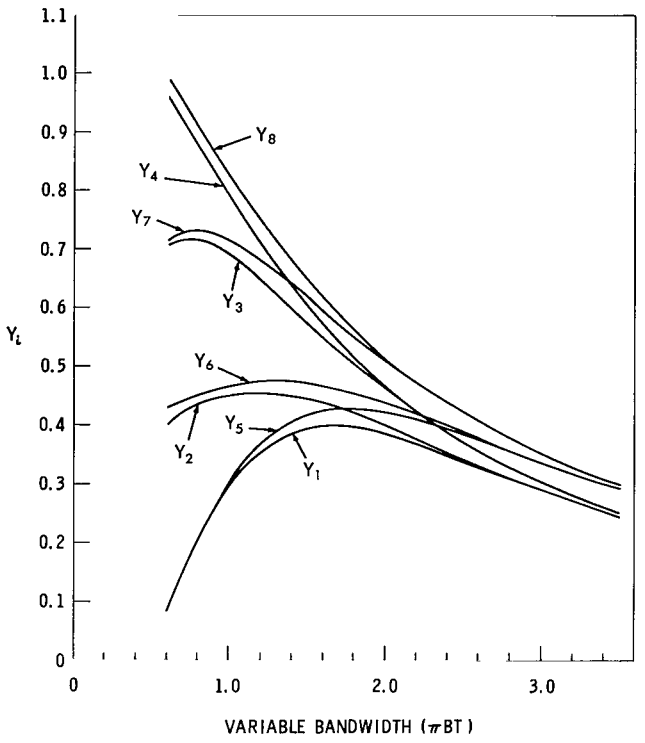

Figure 5—The plot of Y_i vs. πBT for the singly tuned filter case.

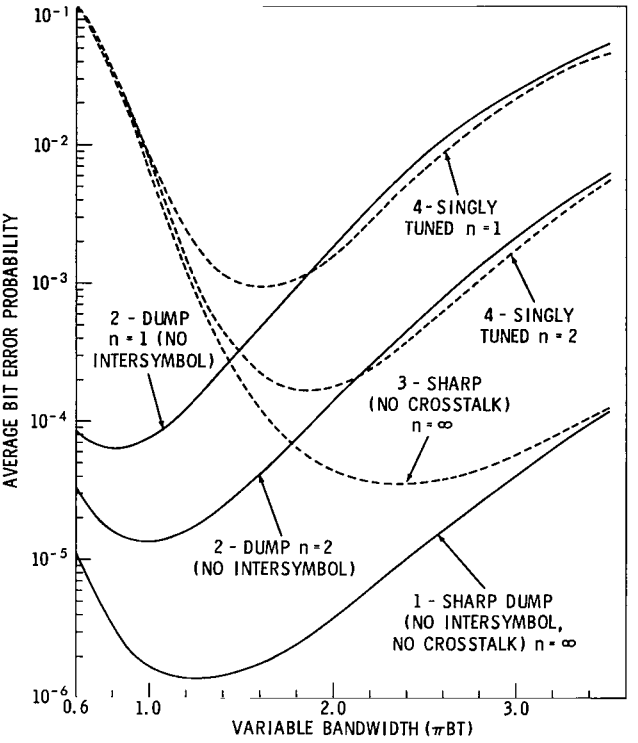

Figure 6—Bit error probability vs. πBT for an $(S/N)_{in}$ of 13 db.

behavior of $\langle P \rangle$ for the four cases by examining the variation of $(Y_1 + Y_5)/2$, as is done in Figure 3. The above conjecture is proven true by observing in Figure 4 that for a <1.6

$$\frac{P_1 + P_5}{8} \approx \frac{1}{8}\sum_{i}^{8} P_i \quad . \tag{16}$$

The relations expressed by Equations 12, 13, 14, and 7 and 12 are plotted in Figures 6 and 7 for S/N = 13 and 16 db, respectively. From Figures 6 and 7 one may observe that the optimum πBT for a singly tuned filter varies from 1.6 (n = 1) to 2.3 (n = ∞). The optimum πBT for a dump type filter varies from .8 to 1.3.

The locations of the minimum P_e are affected very little by the $(S/N)_{in}$.

DISCUSSION

The average probability of error for the FSK system described in Figure 1 is given by Equation 5 as

$$\langle P \rangle = \sum_{i=1}^{2^k} P(i)\,(P_e)_i = \frac{1}{2}\sum_{i=1}^{2^k} P(i)\, e^{-\pi/2(E/N_0)_{in} Y_i^2} \quad . \tag{17}$$

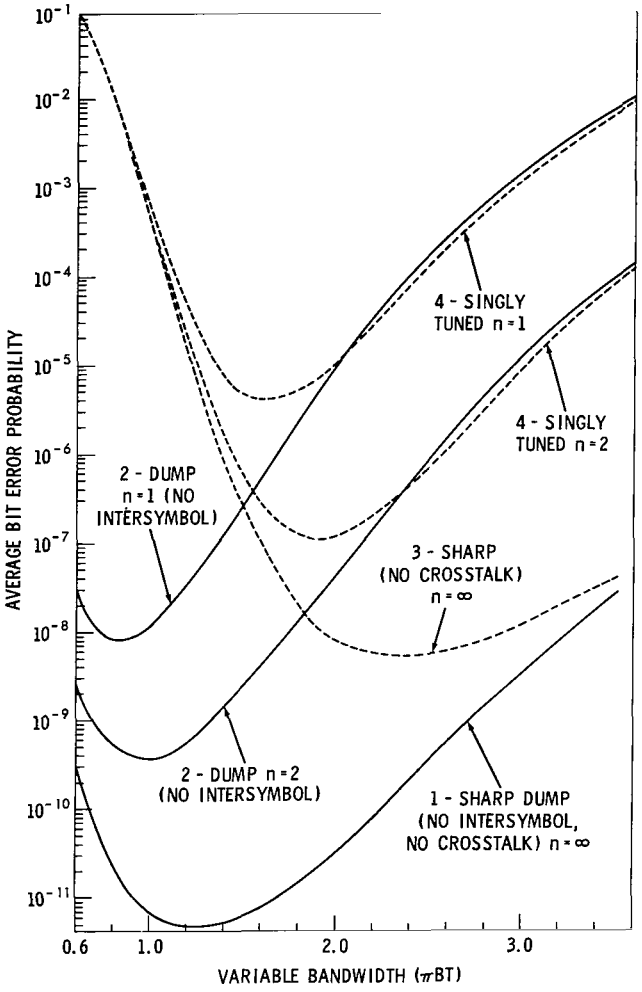

Figure 7—Bit error probability vs. πBT for an $(S/N)_{in}$ of 16 db.

where Y_i is a function of the binary sequence input of length k. Each Y_i is in turn a function of two important parameters, the intersymbol interference and the crosstalk.

The intersymbol interference becomes evident as the sum of one or more terms of the form e^{-ka} as seen in Equation 8c.

The crosstalk is in the form of a factor multiplied by $1/D_2^2$ or $1/D_1^2$, depending on whether this crosstalk is referred to the mark or space filter.

For large D, $1/D_i$ is inversely proportional to n, the ratio of the frequency separation of the shift frequencies to the data rate.

For normal values of a and n Equation 12 yields curves 4 (Figures 3, 6, and 7) which represent the actual case of a singly tuned filter.

In curve 3 of these figures, n is allowed to approach infinity, which is equivalent to either increasing the separation so that $(f_1 - f_2)/f_D$ is very large, or using very sharp filters (rectangular in the limit) with n in the order of 5. Either of the above techniques will eliminate crosstalk and is equivalent to $n = \infty$.

In curve 2 of these figures, n is back to normal but the exponential terms are eliminated, giving us the case of no intersymbol interference usually accomplished by dump filters. Finally, curve 1 of these figures represents the case of no crosstalk and no intersymbol interference.

The relations resulting from the above modifications are given by Equations 9 through 12.

It would be of interest to examine the asymptotic relations of the above four cases.

As a *approaches zero*, $1/D_i \to 0$ and

$$\text{(a)} \qquad Y_i = \lim_{a \to 0} \frac{1 - e^{-a}}{\sqrt{a}} = \lim_{a \to 0} \sqrt{a} \left(1 - \frac{as}{2!} + \frac{a^2}{3!} - + \cdots\right) = 0 \qquad a = \pi BT \tag{18}$$

for cases 1 and 2 and for all i.

(b) Y_i approaches zero for cases 3 and 4 in a similar manner as seen from the respective Equations 9 through 12.

The similarities indicated in part (a) for curves 1 and 2, and in (b) for 3 and 4 are demonstrated in Figures 3, 6, and 7. The explanation lies in the fact that for very small values of a, intersymbol interference is solely responsible for the behavior of the output. Consequently, 1 and 2 may be classified as similar in the fact that they are both independent of intersymbol interference. On the other hand, curves 3 and 4 both depend on intersymbol interference, and therefore, vary similarly at low values of a.

As a *approaches infinity*, a similar behavior may be observed for curves 1 and 3, and for curves 2 and 4 for large values of a. The explanation this time lies in the fact that for large a, the behavior of the curves is mainly influenced by crosstalk.

In summarizing the filter performance, one may reclassify these four filters in this manner:

(a) The filter of case 2 is of the dump type, thus completely eliminating the intersymbol interference.

(b) The filter of case 3 completely eliminates subcarrier crosstalk.

(c) The filter of case 1 is both sharp and of the dump type, thus combining all the good qualities of filters 2 and 3. Consequently, this filter is superior to both filters 2 and 3, as seen in Figure 3, with data for filters 2 and 3 being the lower bounds at the extreme points of the figure.

(d) The filter of case 4 is a singly tuned filter with *no* dumping. This filter is inferior to either filters 2 or 3, the data for which are the upper bounds at the extreme points of Figure 3. It is of interest to notice that the optimum πBT for this filter occurs at approximately the crossover point of filters 2 and 3, in Figure 3.

CONCLUSIONS

The results of this study are graphically shown in Figures 6 and 7, from which the following conclusions may be drawn.

For a given n (subcarrier separation to data rate ratio) the dump type filters are superior, and the optimum πBT ranges from .8 at $n = 1$ to 1.3 at $n = \infty$.

Similarly the optimum πBT for a singly tuned filter ranges from 1.6 ($n = 1$) to 2.3 ($n = \infty$).

The values of πBT, corresponding to the minimum points of the six curves in Figure 6, are approximately the same of those in Figure 7, indicating very little dependence of the minimum points on the $(S/N)_{in}$.

The improvement obtained by the transition from $n = 1$ to $n = 2$ is almost as much as the improvement from $n = 2$ to $n = \infty$. This implies that although an increase in n (or equivalently the

use of sharper filters) will improve the system, one should not use n's larger than 3 as the improvement above this point is of no real value.

Another conclusion that may be drawn from Figures 4 and 5 is the unequal weights of the probabilities of error due to the different inputs $(P_1, \ldots, P_8)$, and specifically the proximity of the $(P_1 + P_5)/8$ curves to the $\langle P \rangle$ curve.

This inequality of the P_i's and the fact that the main contributions to $\langle P \rangle$ are derived from only two out of eight inputs for a certain range of πBT suggests a possible improvement in the system by controlling the source symbol probability.

(Manuscript received January 14, 1965)

REFERENCES

1. Lawton, J. G., "Comparison of Binary Data Transmission Systems," In: *"Second National Convention on Military Electronics, June 16-18, 1958, Washington; Proceedings,"* (Professional Group on Military Electronics, Institute of Radio Engineers, sponsors) Washington: McGregor and Werner, Inc., 1958, pp. 54-61.

2. Glenn, A. B., "Performance Analysis of a Data Link System," *IRE Trans. Comm. Systems,* 7(1):14-24, May 1959.

BIBLIOGRAPHY

Davenport, W. B., and Root, W. L., "An Introduction to the Theory of Random Signals and Noise," New York: McGraw-Hill Book Co., Inc., 1958.

Helstrom, C. W., "Statistical Theory of Signal Detection," New York: Pergamon Press, Inc., 1960.

Schwartz, M., "Information Transmission, Modulation, and Noise; a Unified Approach to Communication Systems," New York: McGraw-Hill Book Co., Inc., 1959.

Woodward, P. M., "Probability and Information Theory, with Applications to Radar," New York: Pergamon Press, Inc., 1953.

Sunde, E. D., "Ideal Binary Pulse Transmission by AM and FM," *Bell System Tech. J.* 38(6):1357-1426, November 1959.

Bennett, W. R., and Rice, S. O., "Spectral Density and Autocorrelation Functions Associated with Binary Frequency-Shift Keying," *Bell System Tech. J.* 42(5):2355-2385, September 1963.

Doelz, M. L., Heald, E. T., and Martin, D. L., "Binary Data Transmission Techniques for Linear Systems," *Proc. I.R.E.* 45(5, Pt. 1):656-661, May 1957.

Lawton, J. G., "Theoretical Error Rates of 'Differentially Coherent' Binary and 'Kineplex' Data Transmission Systems," *Proc. I.R.E.* 47(2):333-334, February 1959.

Davey, J. R., and Matte, A. L., "Frequency Shift Telegraphy — Radio and Wire Applications," *Am. Inst. Electr. Engrs. Trans.* 66:479-494, 1947.

Bennett, W. R., Curtis, H. E., and Rice, S. O., "Interchannel Interference in FM and PM Systems under Noise Loading Conditions," *Bell System Tech. J.* 34(3):601-636, May 1955.

Sunde, E. D., "Theoretical Fundamentals of Pulse Transmission. I," *Bell System Tech. J.* 33(3):721-788, May 4, 1954, and "---II," *BSTJ* 33(4):987-1010, July 1954.

Gardner, M. F., and Barnes, J. F., "Transients in Linear Systems," New York: John Wiley & Sons, 1942. Appendix A.

Appendix A

A Low-Pass to Band-Pass Filter Equivalence

This appendix is to show the equivalence of the envelope of the response of band-pass filters to an amplitude modulated signal, with the response of an equivalent low-pass filter to the envelope of the amplitude modulated signal (Figures A1a and A1b).

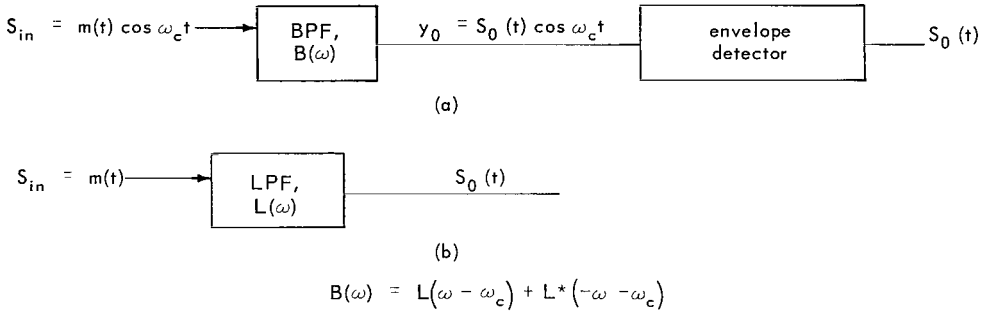

$$B(\omega) = L(\omega - \omega_c) + L^*(-\omega - \omega_c)$$

Figure A1—Band-pass to low-pass equivalence.

Preliminary Examination

$$\{\text{Re } H(\omega)\} = H(\omega) + H^*(\omega) \tag{A1}$$

If $H(s)$ is the transfer function of a physically realizable network, it is a positive real function.*

If $\sigma = 0$, then $H(s)$ may be represented by

$$H(\omega) = \frac{A(\omega) + jB(\omega)}{C(\omega) + jD(\omega)}$$

where A, C are polynominals of even powers of ω and B, D are functions of odd powers of ω. $H(\omega)$ is also

$$H(\omega) = \frac{A(\omega) + j\omega N(\omega)}{C(\omega) + j\omega G(\omega)}$$

*$\text{Re}\{H(s) \geq 0\}$ if $\sigma \geq 0$ where $s = \sigma + j\omega$.

where all A, N, C, G are polynomials of even powers of ω. Rationalizing this function, we have

$$H(\omega) = \frac{[AC + \omega^2 NG + j\omega(NC - AG)]}{C^2 + \omega^2 G^2} . \tag{A2}$$

Thus one may express $H(\omega)$ as a function of the polynomials P_1, P_2, P_3 of even powers of ω, so

$$H(\omega) = \frac{P_1(\omega) + j\omega P_2(\omega)}{P_3(\omega)} = E(\omega) + jO(\omega) . \tag{A3}$$

Then

$$H^*(\omega) = \frac{P_1(\omega) - j\omega P_2(\omega)}{P_3(\omega)} , \tag{A4}$$

where $P(\omega) = P(-\omega)$ if P is a polynomial of even powers of ω.

Adding $H(\omega)$ and its conjugate yields

$$H(\omega) + H^*(\omega) = 2\mathrm{Re}\{H(\omega)\} . \tag{A5}$$

The conclusion of the above preliminary examination is that the real part of $H(\omega)$ is equal to one half the sum of $H(\omega)$ and its conjugate.

Examination of High-Q Band-Pass Filter

Consider the high Q band-pass filter $B(\omega)$ which is symmetrical amplitude-wise $[|B(\beta+\alpha)| = |B(\beta-\alpha)|]$ and antisymmetric phase-wise $[\phi(\omega) = \phi_0(\omega-\beta) \sim \omega-\beta]$ about some frequency.

The transfer function of such a band-pass filter may be expressed in terms of a low-pass filter as: $B(\omega) = L(\omega-\beta) + L^*(-\omega-\beta)$.

The impulse response of $B(\omega)$ then becomes

$$b(t) = F^{-1}\{B(\omega)\} = \int_{-\infty}^{\infty} B(\omega)\, e^{j\omega t}\, df$$

$$= \frac{1}{2\pi}\left[\int_{-\infty}^{\infty} L(\omega-\beta)\, e^{j\omega t}\, d\omega + \int_{-\infty}^{\infty} L^*(-\omega-\beta)\, e^{j\omega t}\, d\omega\right] . \tag{A6}$$

If $x = \omega - \beta$ and $y = -\omega - \beta$, then

$$b(t) = \frac{1}{2\pi}\left[\int_{-\infty}^{\infty} L(x)\, e^{j(x+\beta)t}\, dx + \int_{-\infty}^{\infty} L^*(y)\, e^{-j(y+\beta)t}\, dy\right] . \tag{A7}$$

Letting the variable $y \rightarrow x$, we have

$$b(t) = \frac{1}{2\pi}\left[\int_{-\infty}^{\infty} L(x)\, e^{j(x+\beta)t}\, dx + \int_{-\infty}^{\infty} L^*(x)\, e^{-j(x+\beta)}\, dx\right]$$

$$= e(t)\, e^{j\beta t} + e^*(t)\, e^{-j\beta t}$$

$$= 2\mathrm{Re}\left\{e(t)\, e^{j\beta t}\right\} . \tag{A8}$$

Conclusion:

If $e(t)$ is considered as a complex envelope of the impulse response of the bandpass filter $b(t)$, then this envelope is the inverse Fourier transform of the equivalent low pass filter.

Now we may prove the equivalence of the two cases illustrated in Figure A1. The response in Figure A1b is:

$$S_0(t) = \int_0^{\infty} e(\tau)\, m(t-\tau)\, d\tau , \tag{A9}$$

where

$$e(\tau) = \frac{1}{2\pi}\int_{-\infty}^{\infty} L(\omega)\, e^{j\omega\tau}\, d\omega . \tag{A10}$$

For the case of Figure A1a:

$$y_0(t) = \int_0^\infty b(\tau)\, S_{in}(t-\tau)\, d\tau$$

$$= \int_0^\infty b(\tau)\, m(t-\tau)\, \mathrm{Re}\left\{e^{j\omega_c(t-\tau)}\right\} d\tau$$

$$= 2\int_0^\infty \mathrm{Re}\left\{e(\tau)\, e^{j\beta\tau}\right\} m(t-\tau)\, \mathrm{Re}\left\{e^{j\omega_c(t-\tau)}\right\} d\tau$$

$$= \frac{1}{2}\int_0^\infty \left[e(\tau)\, e^{j\beta\tau} + e^*(\tau)\, e^{-j\beta\tau}\right]\left[e^{j\omega_c(t-\tau)} + e^{-j\omega_c(t-\tau)}\right] d\tau$$

$$= \frac{1}{2}\int_0^\infty e(\tau)\, e^{j\omega_c t}\, m(t-\tau)\, e^{j(\beta-\omega_c)\tau}\, d\tau + \frac{1}{2}\int_0^\infty e^*(\tau)\, e^{j\omega_c t}\, m(t+\tau)\, e^{-j(\beta+\omega_c)\tau}\, d\tau$$

$$+ \frac{1}{2}\int_0^\infty e(\tau)\, e^{-j\omega_c t}\, m(t-\tau)\, e^{j(\beta+\omega_c)\tau}\, d\tau + \frac{1}{2}\int_0^\infty e^*(\tau)\, e^{-j\omega_c t}\, m(t-\tau)\, e^{-j(\beta-\omega_c)\tau}\, d\tau. \quad \text{(A11)}$$

When $y_0(t)$ is passed through an envelope detector, it virtually eliminates the higher frequencies and if $\omega_c = \beta$, then

$$y_0(t) = \frac{1}{2}\int_0^\infty e(\tau)\, e^{j\omega_c t}\, m(t-\tau)\, d\tau + \frac{1}{2}\int_0^\infty e^*(\tau)\, e^{-j\omega_c t}\, m(t-\tau)\, d\tau$$

$$= \int_0^\infty \mathrm{Re}\left\{e(\tau)\, e^{j\omega_c t}\right\} m(t-\tau)\, d\tau\ . \quad \text{(A12)}$$

If $e(\tau)$ is real† then

$$y_0(t) = \cos\omega_c t \int_0^\infty e(\tau)\, m(t-\tau)\, d\tau \quad \text{(A13)}$$

and

$$S_0(t) = \int_0^\infty e(\tau)\, m(t-\tau)\, d\tau\ . \quad \text{(A14)}$$

†This implies symmetry of $B(\omega)$ about β or high Q.

For a singly tuned circuit of Figure E1 (Appendix E),

$$B(\omega) = \frac{j2a\omega}{-\omega^2 + 2ja\omega + \beta_0^2} = \frac{-j2a\omega}{(\omega + \beta - ja)(\omega - \beta - ja)}$$

$$= \frac{-a(a + j\beta)}{\beta(\omega + \beta - ja)} + \frac{a(a - j\beta)}{\beta(\omega - \beta - ja)} , \qquad \text{(A15)}$$

where

$$\beta^2 = \beta_0^2 - a^2 , \qquad a = \frac{1}{2RC} , \qquad \beta_0 = \frac{1}{\sqrt{LC}} .$$

So we have as a result

$$B(\omega) = \frac{a(a + j\beta)}{\beta(-\omega - \beta + ja)} + \frac{a(a - j\beta)}{\beta(\omega - \beta - ja)} . \qquad \text{(A16)}$$

The first term may be identified as $L^*(-\omega - \beta)$ and the second term as $L(\omega - \beta)$; so

$$L(\omega) = \frac{a(a - j\beta)}{\beta(\omega - ja)} . \qquad \text{(A17)}$$

Then

$$e(t) = \frac{a(ja + \beta)}{\beta} \frac{1}{2\pi} \int_{-\infty}^{\infty} \frac{e^{j\omega t}\, d\omega}{j(\omega - ja)}$$

$$= \frac{a(ja + \beta)\, e^{-at}}{\beta} \frac{1}{2\pi} \int_{-\omega}^{\infty} \frac{e^{j(\omega - ja)t}\, d(\omega - ja)}{j(\omega - ja)} \, d\omega$$

$$= \frac{a}{\beta} (ja + \beta)\, e^{-at} . \qquad \text{(A18)}$$

For a high Q circuit $a \ll \beta$ and

$$e(t) = ae^{-at} , \qquad \text{(A19)}$$

which is identified as the impulse response of a low pass filter with a time constant equal to 2RC.

Appendix B

The Step Response of a Singly-Tuned Circuit

The usefulness of the step response of a singly tuned circuit becomes apparent when rectangular envelopes are used as inputs.

For example, let $S_{in}(t) = \text{rect}(T)\sin\omega t$ where

$$\text{rect}(T) \begin{cases} = U(t) & 0 \le t \le T \\ = U(t) - U(t-T) = 0 & t > T \end{cases}$$

and $\sin\omega t$ is replaced by its exponential form.

The Laplace Transform of the Input is

$$S(s) = \frac{1}{2j}\int_0^\infty \text{rect}(T)\left[e^{j\omega t} - e^{-j\omega t}\right] e^{-st}\, dt$$

$$= \frac{1}{2j}\left[\text{rect}(s - j\omega, T) - \text{rect}(s + j\omega, T)\right]$$

$$= \frac{1}{2j}\left[\frac{1 - e^{-(s-j\omega)T}}{s - j\omega} - \frac{1 - e^{-(s+j\omega)T}}{s + j\omega}\right]$$

$$= \frac{\omega}{s^2 + \omega^2} - \frac{e^{-sT}}{s^2 + \omega^2}\left[s\sin\omega T + \omega\cos\omega T\right]. \qquad \text{(B1)}$$

The first term is the beginning of the rectangle and the last term is the end of the rectangular wave. For $0 < t < T$ the second term vanishes.

Response for $0 < t < T$

$$Y(s) = S(s)H(s) = \frac{\omega}{s^2 + \omega^2}\,\frac{2\alpha s}{(s+\alpha)^2 + \beta^2}. \qquad \text{(B2a)}$$

Expanding by partial fractions yields

$$\frac{\omega}{s^2 + \omega^2}\,\frac{2\alpha s}{(s+\alpha)^2 + \beta^2} = \frac{As + B}{s^2 + \omega^2} + \frac{C(s + a_0)}{(s+\alpha)^2 + \beta^2}, \qquad \text{(B2b)}$$

where

$$\left.\begin{aligned} A &= \frac{2a\omega\left(\beta_0^2 - \omega^2\right)}{\left(\beta_0^2 - \omega^2\right)^2 + 4a^2\omega^2} = \frac{2a\omega\left(\beta_0^2 - \omega^2\right)}{K^2} \\ B &= A\,\frac{2a\omega^2}{\beta_0^2 - \omega^2} \\ C &= -A \end{aligned}\right\} \qquad \text{(B2c)}$$

$$a_0 = \frac{2a\beta_0^2}{\beta_0^2 - \omega^2} \,. \qquad \text{(B2d)}$$

Then $y(t)$ is*

$$y(t) = A\cos\omega t + \frac{B}{\omega}\sin\omega t + \frac{C\left[\left(a_0 - a\right)^2 + \beta^2\right]^{1/2}}{\beta}\, e^{-at}\sin\left(\beta t + \psi\right) , \qquad \text{(B3a)}$$

where

$$\psi = \tan^{-1}\frac{\beta}{a_0 - a} = \tan^{-1}\frac{\beta\left(\beta_0^2 - \omega^2\right)}{a\left(\beta_0^2 + \omega^2\right)} \,. \qquad \text{(B3b)}$$

Now,

$$\begin{aligned} \sin\left(\beta t + \psi\right) &= \sin\left[\left(\beta t + \psi - \omega t\right) + \omega t\right] \\ &= \sin\left[\left(\beta - \omega\right) t + \psi\right]\cos\omega t + \cos\left[\left(\beta - \omega\right) t + \psi\right]\sin\omega t \end{aligned} \qquad \text{(B4)}$$

and

$$C\left[\left(a_0 - a\right)^2 + \beta^2\right]^{1/2} = -\frac{A}{\beta_0^2 - \omega^2}\,\beta_0 K \,. \qquad \text{(B5)}$$

*Gardner, M. F., and Barnes, J. F., "Transients in Linear Systems," New York: John Wiley & Sons, 1942. Appendix A.

By making the appropriate substitutions for A, B, C and a_0 of Equations B3c and B4 into Equation B3a, then Equation B3a becomes

$$y(t) = \frac{2a\omega}{K^2}\left\{\left(\beta_0^2-\omega^2\right)\cos\omega t + 2a\omega\sin\omega t - \frac{\beta_0 K e^{-at}}{\beta}\sin\left[(\beta-\omega)\,t+\psi\right]\cos\omega t - \frac{\beta_0 K e^{-at}}{\beta}\cos\left[(\beta-\omega)\,t+\psi\right]\sin\omega t\right\}$$

$$= \frac{2a\omega}{K^2}\sin(\omega t+\theta)\sqrt{\left\{2a\omega - \frac{\beta_0 K}{\beta}e^{-at}\cos[]\right\}^2 + \left\{\beta_0^2-\omega^2-\frac{\beta_0}{\beta}Ke^{-at}\sin[]\right\}^2}$$

$$= \frac{2a\omega}{K^2}\sin(\omega t+\theta)\sqrt{K^2+\left(\frac{\beta_0}{\beta}Ke^{-at}\right)^2 - 2\frac{\beta_0}{\beta}Ke^{-at}\left\{2a\omega\cos[]+\left(\beta_0^2-\omega^2\right)\sin[]\right\}}$$

$$= \frac{2a\omega}{K}\sin(\omega t+\theta)\sqrt{1+\left(\frac{\beta_0}{\beta}e^{-at}\right)^2 - \frac{2\beta_0}{\beta}e^{-at}\cos\left[(\beta-\omega)\,t+\psi-\phi\right]}\,, \tag{B6}$$

where

$$K^2 = \left(\beta_0^2-\omega^2\right)^2 + 4a^2\omega^2\,, \tag{B7}$$

$$\theta = \tan^{-1}\frac{2a\omega - K\frac{\beta_0}{\beta}e^{-at}\cos\left[(\beta-\omega)\,t+\psi\right]}{\beta_0^2-\omega^2-\frac{K\beta_0}{\beta}e^{-at}\sin\left[(\beta-\omega)\,t+\psi\right]}\,, \tag{B8}$$

$$\phi = \tan^{-1}\frac{2\beta_0^2-\omega^2}{4a\omega}\,. \tag{B9}$$

Now

$$\frac{2a\omega}{K} = \frac{2a\omega}{\left(\beta_0^2-\omega^2\right)^2+4^2a^2\omega^2} = \frac{1}{\left(\frac{\beta_0^2-\omega^2}{2a\omega}\right)^2+1}\,. \tag{B10}$$

So letting $a = \pi B$, as found in Appendix E, the envelope of the output is:

$$e(t) = \frac{1}{\sqrt{\left(\frac{\beta_0^2-\omega^2}{2\pi B\omega}\right)^2+1}}\sqrt{\left(1-\frac{\beta_0}{\beta}e^{-\pi Bt}\right)^2 + 4\frac{\beta_0}{\beta}e^{-\pi BT}\sin^2\left[\frac{(\beta-\omega)\,t}{2}+\frac{\psi-\phi}{2}\right]}\,, \tag{B11}$$

where $\beta - \omega$ is the frequency offset. When $\beta - \omega = 0$, then

$$e(t) = \frac{1}{\sqrt{\left(\frac{\pi B}{2\beta}\right)^2 + 1}} \left[1 - \frac{\beta_0}{\beta} e^{-\pi Bt}\right] \cong 1 - de^{-\pi Bt} , \tag{B12}$$

where $d = \beta_0/\beta$.

Response for $t > T$

The response for this case is the same as for the rising end of the rectangle except for the sign. For the simple case of no offset

$$e(t) = V_0 de^{-\pi B(t-T)} = \left(1 - de^{-\pi BT}\right) de^{-\pi B(t-T)} , \tag{B13}$$

where V_0 is the initial condition.

A simpler derivation of the above expression is given in Appendix A.

Appendix C

Generalized Filter Outputs in the FSK System

Using the results of Appendix B, the output of the mark filter $y(t)$, due to a mark frequency $(\omega_1 = \beta_1)$ applied during the first period $(0 < t < T)$ and expressed by

$$\left[u(t) - u(t-T)\right] \sin \omega_1 t \ ,$$

is, assuming $\pi B^2/2\beta_1 << 1$, equal to*

$$y_{mm}(t) = \left(1 - d_1 e^{-\pi BT}\right) d_1 e^{-\pi B(t-T)} \sin \omega_1\left(t + \theta_1\right) . \tag{C1}$$

So the output at the k^{th} sampling instant $(t = kT)$ is:

$$y_{mm}(kT) = y_{mmk} = \left(1 - d_1 e^{-a}\right) d_1 e^{-a(k-1)} \sin\left(\omega_1 t + \theta_1\right) \qquad K \geq 1 . \tag{C2}$$

Similarly, the output of the mark filter due to a rectangular input of a space frequency, ω_2 of the form

$$\left[u(t) - u(t-T)\right] \sin \omega_2 t$$

is:

$$y_{ms} = \left[\frac{\left(1 - de^{-\pi Bt}\right)^2 + 4de^{-\pi Bt} \sin^2 \dfrac{\beta_1 - \omega_2 + \psi - \phi}{2}}{\left(\dfrac{\beta_1^2 - \omega_2^2}{2\pi B\omega_2}\right)^2 + 1}\right]^{1/2} \sin\left(\omega_2 t + \theta_2\right) . \tag{C3}$$

The envelope of the above term is much smaller than y_{mm} and is identified as the crosstalk.

The sinusoidal term in Equation C3 indicates that the crosstalk is periodic with a period $1/\Delta f_1$ where Δf_1 is the difference between the space frequency and the mark filter center frequency, $(\beta_1 - \omega_2)/2\pi$. Similarly, the crosstalk in the space filter would have a Δf_2 equal to the difference of the mark frequency and the space filter center frequency, $(\beta_2 - \omega_1)/2\pi$.

*The first subscript refers to the mark filter and the second to the waveform applied; also see Figure 1.

The crosstalk amplitude is bounded by the expression

$$\frac{1 \mp d_1 e^{-\pi B t}}{\left[\left(\frac{\beta_1^2 - \omega_2^2}{2\pi B \omega_2}\right)^2 + 1\right]^{1/2}} \quad . \tag{C4}$$

If $\beta_1 - \omega_2 = 2\pi f_D$ is the data rate, then the period of the envelope of the above term will be equal to the period of the data rate, with maxima and minima indicated in Equation C4.

Assuming, for the time being, that the sampling coincides with the minimum value of the expression of Equation C4, the crosstalk at the k^{th} sampling instant is given by

$$y_{ms}(kT) = y_{msk} = \frac{\left(1 - d_1 e^{-a}\right) d_1 e^{-a(k-1)}}{\left[\left(\frac{\beta_1 + \omega_2}{\omega_2}\right)^2 \left(\frac{\beta_1 - \omega_2}{2\pi B}\right)^2 + 1\right]^{1/2}} \sin\left(\omega_2 t + \theta_2\right) \text{ with } k \geq 1 \; . \tag{C5}$$

Up to now, y_{--k} is the response at the k^{th} sampling instant ($t = kT$) due to a signal applied during the first period as shown in Figure C1.

In general, the response at the k^{th} sampling instant due to a waveform applied during the j^{th} period is identical to that given by Equations B12 and C5 with $k - 1$ replaced by $k - j$.

Furthermore, $y_{s,s,k-j}$ and $y_{s,m,k-j}$ are identical to $y_{m,m,k-j}$ and $y_{m,s,k-j}$ with the subscripts 1 and 2 interchanged, respectively. Consequently, we have

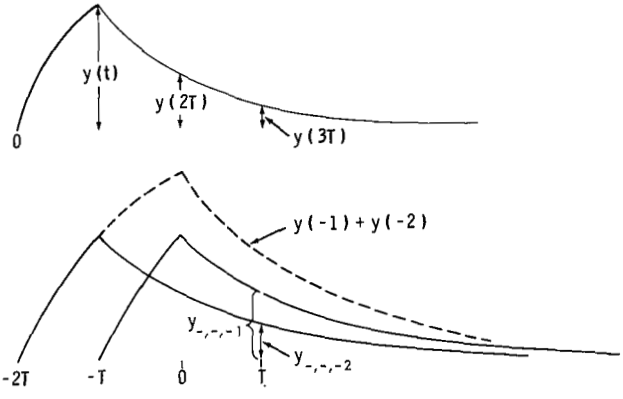

Figure C1—Sketches of the response of a low-pass filter to a square U(t) - U(t - T), and to two consecutive square pulses of the combined form U(t + 2T) - U(t).

$$\left.\begin{aligned}
y_{m,m,k-j} &= \left(1 - d_1 e^{-a}\right) d_1 e^{-a(k-j)} \sin\left(\omega_1 t + \theta_1\right) , \\
y_{m,s,k-j} &= \frac{\left(1 - d_1 a^{-a}\right) d_1 e^{-a(k-j)}}{D_1} \sin\left(\omega_2 t + \theta_3\right) , \\
y_{s,s,k-j} &= \left(1 - d_2 e^{-a}\right) d_2 e^{-a(k-j)} \sin\left(\omega_2 t + \theta_2\right) , \\
y_{s,m,k-j} &= \frac{\left(1 - d_2 e^{-a}\right) d_2 e^{-a(k-j)}}{D_2} \sin\left(\omega_1 t + \theta_4\right) ,
\end{aligned}\right\} \tag{C6}$$

where $k \geq j$ and D_2 is clear from Equation C5 and the statement following Equation C5.

Referring to Figure C1, we see that

$$y_{1K}^2 = \left[\sum_{j=-\infty}^{k} b_j\, y_{m,m,k-j}\right]^2 + \left[\sum_{j=-\infty}^{k} (1-b_j)\, y_{m,s,k-j}\right]^2 \tag{C7}$$

where $b_j = 1, 0$ and $k \geq j$.

Obviously, since the signal at the j^{th} interval is either a mark or a space, one or the other of the above terms must equal to zero for a given j; this is taken into consideration by letting b_j equal 1 if the digit of the j^{th} interval is a mark, and zero if it is a space. Similarly,

$$y_{2k}^2 = \left[\sum_{j=-\infty}^{k} b_j\, y_{s,m,k-j}\right]^2 + \left[\sum_{j=-\infty}^{k} (1-b_j)\, y_{s,s,k-j}\right]^2 . \tag{C8}$$

Appendix D

Comparator Output Signal-to-Noise Ratios

The general expression for Y_1 is given by the equation below:

$$Y_1 = \frac{1 - e^{-a}}{\sqrt{a}} \left\{ \left[\left(\frac{e^{-a} + e^{-2a}}{D} \right)^2 + 1 \right]^{1/2} - \left[\left(e^{-a} + e^{-2a} \right)^2 + \frac{1}{D^2} \right]^{1/2} \right\} \tag{D1}$$

where $e^{-a} + e^{-2a}$ is intersymbol interference and $\left(e^{-a} + e^{-2a}\right)^2 + 1/D^2$ is the crosstalk.

1. For a dump type filter all intersymbol interferences vanish and Equation D1 becomes

$$Y_1 = \frac{1 - e^{-a}}{\sqrt{a}} \left(1 - \frac{1}{D}\right) = \frac{1 - e^{-a}}{\sqrt{a}} \left(1 - \frac{a}{\sqrt{k^2 + a^2}}\right) = Y_2 = Y_3 = Y_4 , \tag{D2}$$

where

$$k^2 \quad \frac{(m+1)n\pi}{a} , \qquad m = \frac{\beta_i}{\omega_j} , \qquad n = \frac{\beta_i - \omega_j}{2\pi f_D}$$

2. For dump type filters with large subcarrier separation D becomes very large and Equation D1 reduces to Equation D2, and

$$Y_1 = \frac{1 - e^{-a}}{\sqrt{a}} = Y_2 = Y_3 = Y_4 \tag{D3}$$

3. If sharp filters are used so that D is still large but there is no dumping, then

$$Y_1 = \frac{1 - e^{-a}}{\sqrt{a}} \left(1 - e^{-a} - e^{-2a}\right) , \tag{D4a}$$

$$Y_2 = \frac{1 - e^{-a}}{\sqrt{a}} \left(1 + e^{-2a} - e^{-a}\right) , \tag{D4b}$$

$$Y_3 = \frac{1 - e^{-a}}{\sqrt{a}} \left(1 + e^{-a} - e^{-2a}\right) , \tag{D4c}$$

and

$$Y_4 = \frac{1 - e^{-a}}{\sqrt{a}} \left(1 + e^{-a} + e^{-2a}\right) . \qquad \text{(D4d)}$$

The relations represented by Equations D1, D2, D3, and D4 have been plotted in Figures 3a and 3b.

Appendix E

Formulation of the Expressions Governing A Singly Tuned Circuit

The transfer function of a circuit of Figure E1 is:

$$H(s) = \frac{\frac{S}{RC}}{s^2 + \frac{1}{LC} + \frac{1}{RC}} . \tag{E1a}$$

If we let $\alpha = 1/(2RC)$, $\beta_0^2 = 1/(LC)$, $\beta^2 = \beta_0^2 - \alpha^2$ and $s = j\omega$, then

$$H(\omega) = \frac{j2\alpha\omega}{-\omega^2 + \beta_0^2 + j2\alpha\omega} = \frac{-j2\alpha\omega}{\omega^2 - j2\alpha\omega - \beta_0^2} . \tag{E1b}$$

To solve for the bandwidth, B, we must find the 3 db frequencies ω_1, $\omega_2 = \beta_0 \pm \Delta$ by using Equation E2a:

$$\left|H(\beta_0)\right|^2 = 2\left|H(\beta_0 \pm \Delta)\right|^2 . \tag{E2a}$$

Putting $H(\omega)$ in a more convenient form gives

$$H(\omega) = \frac{2\alpha}{j\left(\omega - \frac{\beta_0^2}{\omega}\right) + 2\alpha} , \tag{E2b}$$

and we may find that

$$1 = \frac{2(2\alpha)^2}{(2\alpha)^2 + \left[(\beta_0 \pm \Delta) - \frac{\beta_0^2}{(\beta_0 \pm \Delta)}\right]^2} . \tag{E3}$$

By rearranging terms, we have

$$\alpha^2 (\beta_0 \pm \Delta)^2 = \Delta^2 \left(\beta_0 \pm \frac{\Delta}{2}\right)^2 . \tag{E4}$$

For a high Q filter $\beta_0 \gg \Delta$, $(\beta_0 > 10\Delta)$, and $\Delta \simeq \alpha$. Then $2\pi B = 2\Delta = 2\alpha$ (radians) and $B = \alpha/\pi$.

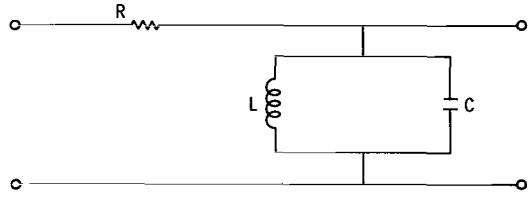

Figure E1—Singly tuned circuit, where R represents the combination of the source output resistance and the coil equivalent resistance.

Appendix F

Definitions

$a = \pi BT$

B = The 3 db bandwidth

$d_i = \frac{\beta_{0i}}{\beta_i} \cong 1 + \frac{\alpha}{\beta_i}$

E = The average signal energy per bit

f_D = The data frequency = $1/T$

$m_1 = \frac{\beta_1}{\omega_2}$; $m_2 = \frac{\beta_2}{\omega_1}$

N_0 = The noise power density per unit bandwidth

$n = \frac{|\beta_1 - \omega_2|}{2\pi f_D} = \frac{|\beta_2 - \omega_1|}{2\pi f_D}$

$\langle P \rangle$ = The average bit error probability

P_i = The bit error probability corresponding to input i

$P(M)$ = The probability of a mark

$P(S)$ = The probability of a space

$P(M/S)$ = The probability of a space changing to a mark

$P(S/M)$ = The probability of a mark changing to a space

S/N = The signal to noise ratio (average signal power to average noise power)

$\alpha = \frac{1}{2RC} = \pi B$

$\beta = \sqrt{\beta_0^2 - \alpha^2} \cong \beta_0$ for narrow band circuits

$\beta_0 = \frac{1}{\sqrt{LC}}$

β_1 = The resonant frequency of the mark filter (radians/sec)

β_2 = The resonant frequency of the space filter (radians/sec)

ω_1 = The mark frequency (radians/sec)

ω_2 = The space frequency (radians/sec)

"The aeronautical and space activities of the United States shall be conducted so as to contribute . . . to the expansion of human knowledge of phenomena in the atmosphere and space. The Administration shall provide for the widest practicable and appropriate dissemination of information concerning its activities and the results thereof."

—NATIONAL AERONAUTICS AND SPACE ACT OF 1958

NASA SCIENTIFIC AND TECHNICAL PUBLICATIONS

TECHNICAL REPORTS: Scientific and technical information considered important, complete, and a lasting contribution to existing knowledge.

TECHNICAL NOTES: Information less broad in scope but nevertheless of importance as a contribution to existing knowledge.

TECHNICAL MEMORANDUMS: Information receiving limited distribution because of preliminary data, security classification, or other reasons.

CONTRACTOR REPORTS: Technical information generated in connection with a NASA contract or grant and released under NASA auspices.

TECHNICAL TRANSLATIONS: Information published in a foreign language considered to merit NASA distribution in English.

TECHNICAL REPRINTS: Information derived from NASA activities and initially published in the form of journal articles.

SPECIAL PUBLICATIONS: Information derived from or of value to NASA activities but not necessarily reporting the results of individual NASA-programmed scientific efforts. Publications include conference proceedings, monographs, data compilations, handbooks, sourcebooks, and special bibliographies.

Details on the availability of these publications may be obtained from:

SCIENTIFIC AND TECHNICAL INFORMATION DIVISION

NATIONAL AERONAUTICS AND SPACE ADMINISTRATION

Washington, D.C. 20546